Multiple ionization of diatomic molecules in collisions with 50–300-keV hydrogen and helium ions

B. Siegmann,[1] U. Werner,[1] Z. Kaliman,[2] Z. Roller-Lutz,[3] N. M. Kabachnik,[1,*] and H. O. Lutz[1]
[1]*Fakultät für Physik, Universität Bielefeld, D-33615 Bielefeld, Germany*
[2]*Faculty of Philosophy, University of Rijeka, 51000 Rijeka, Croatia*
[3]*Institute of Physics, Faculty of Medicine, University of Rijeka, 51000 Rijeka, Croatia*
(Received 11 August 2002; published 1 November 2002)

Measurements of relative multiple ionization cross sections have been performed for 50–300-keV H^+, D^+, and He^+ impact on N_2, O_2, CO, and NO molecules. Fragment ions with total charges up to $Q=q_1+q_2=5$ have been detected in coincidence using a position- and time-sensitive detector. Dependence of the cross section on the molecular orientation with respect to the ion beam is observed for all targets. The experimental data are compared with theoretical calculations based on the statistical energy deposition model.

DOI: 10.1103/PhysRevA.66.052701 PACS number(s): 34.50.Gb

I. INTRODUCTION

Ionization and fragmentation of diatomic molecules like N_2, O_2, CO, and NO in collisions with light ions (hydrogen and helium) in the keV energy range have been studied for many years (see e.g., [1]). In addition to their fundamental importance for understanding the dynamics of dissociative ionization of multielectron molecules, these studies provide the cross sections that are necessary for modeling planetary and cometary atmospheres and for understanding the processes in natural and man-made plasmas. The proton-impact ionization of these molecules has been investigated mainly in the energy region around and below 100 keV where electron capture contributes considerably to the ionization process: Solov'ev *et al.* [2] measured the cross sections for 10–180-keV $p+N_2$, Browning and Gilbody [3] measured the cross sections for 5–45-keV $p+N_2,O_2,CO$, the collisions of 5–50-keV $p+CO$ were studied by Afrosimov *et al.* [4], Yousif *et al.* [5] measured the cross sections and angular distributions of fragments for 5–25-keV $p+N_2$, and Shah and Gilbody [6] studied 10–98-keV $p+CO$ collisions. Only a few experimental investigations exist for proton-impact ionization at higher energies where direct ionization dominates. Rudd *et al.* [7] measured the total ionization cross section for N_2, O_2, and CO in collisions with 5–4000-keV protons. Electron capture from CO and O_2 molecules was studied by Varghese *et al.* [8] in the energy range 0.8–3.0 MeV. Knudsen *et al.* [9] measured the cross section of single and double ionization of N_2 and CO by impact of 50–6000-keV protons, and Krishnamurthi *et al.* [10] studied the single and multiple ionization of CO by 1-MeV protons.

Similarly, experimental investigations of He ion collisions with N_2, O_2, and CO molecules were mainly performed in the energy region below 100 keV [11–16]. In the high-energy region there are only a few experiments that mostly focus on N_2 molecules: Pivovar *et al.* [17] measured the total ion yield for 200–1800-keV He^+ collisions with N_2, Edwards and Wood studied the dissociative ionization of N_2 in collisions with 1-MeV He^+ ions [18], an electron capture channel with multiple ionization of the molecule was studied in coincidence measurements for 200-keV $He^+ + N_2$ by Ali *et al.* [19], Rudd *et al.* [20] measured the ion production cross sections for collisions of N_2, CO, and O_2 molecules with 10–2000-keV He^+ ions.

In our laboratory the kinetic energy distributions of the molecular fragments were studied for 50–300-keV H^+ and He^+ collisions with N_2 [21–23]. In addition, the angular distributions of molecular fragments were measured for 100–300-keV $He^+ + N_2$ collisions and a strong orientation effect in multiple ionization has been revealed [24]. There are no data for the collisions of H and He ions with NO molecules.

In this paper we present the results of our measurements of the relative cross sections for multiple ionization in collisions of 50–300-keV protons, deuterons, and helium ions with N_2, O_2, CO, and NO molecules. Furthermore, we studied the angular distributions of molecular fragments for each ionization channel. In the axial recoil approximation which is valid for the processes considered the fragment angular distribution gives the dependence of the ionization cross section on the orientation of the molecular axis with respect to the projectile beam at the moment of the collision. We found that for all considered colliding pairs a strong orientation effect exists: the cross section of multiple ionization ($Q>3$) is larger when the molecular axis is aligned along the beam and smaller when it is perpendicular to the beam. This effect, which was theoretically predicted [25,26] and experimentally established for He^+-N_2 collisions [24], is apparently a general feature for all diatomic molecules. It is clearly observed in collision with He^+ ions. For hydrogen ions the observation of the orientation effect is more difficult since the cross sections for multiple ionization are smaller. Nevertheless, as we show below, the orientation effect also exists for hydrogen ions.

We present also theoretical calculations of the multiple ionization cross sections as well as of their orientation dependence. The calculations were performed within the statistical energy deposition (SED) model [27–30]. In the considered energy range the Sommerfeld parameter characterizing the strength of interaction, $\kappa=Z/v$, is about 1 (Z is the projectile charge, v its velocity in atomic units). Thus the energy transfer in the collision cannot be considered in the first-order perturbation theory. We used a recently developed version of the SED model which takes into account higher-order

*On leave from the Institute of Nuclear Physics, Moscow State University, Moscow 119899, Russia.

corrections in the calculations of the energy deposition [31].

In the following section we will briefly describe the experiment. In Sec. III we discuss the relative cross sections of multiple ionization as well as the angular distributions and the orientation effect. The experimental results are compared with the theoretical calculations within the SED model. Some conclusions are formulated in the last section IV.

II. EXPERIMENT

Details of the experimental technique have already been published [32,33]. We therefore give only a brief account of the experimental setup. The collimated beam of 50–300-keV H^+, D^+, or He^+ ions interacts with effusive N_2, O_2, CO, or NO gas targets. The slow ions and electrons generated in the collision process are separated by a weak homogenous electric field of 333 V/cm perpendicular to the detector plane. Electrons are detected by a channeltron at one side of the interaction region; positive ions are accelerated toward the time- and position-sensitive multiparticle detector at the other side. After passing a field-free time-of-flight region the ions are postaccelerated to a few keV to increase the detector efficiency. The detector is based on microchannel plates (MCPs) in combination with an etched crossed-wire anode structure consisting of independent x and y wires [32]: an electron cloud from the microchannel plates hitting a wire crossing will result in coincident pulses on the corresponding x and y wires. For each positive fragment ion the position on the detector (x_i, y_i) and the time of flight t_i relative to the electron signal are recorded. If both fragments from a particular fragmentation are detected these data yield a kinematically complete image of the molecular breakup process, and the dissociation energy and angular correlations can be derived for each individual event. The present experimental setup allows the simultaneous measurement of all reaction channels resulting in at least one electron and one or more positive fragments. In the fast collisions ($\tau_{\mathrm{coll}} < 10^{-16}$ s) considered here ionization and fragmentation may be treated as independent processes. Therefore, in a diatomic molecule the fragment ions emerge in the direction of the molecular axis so that the initial orientation of the molecule at the instance of fragmentation can be derived from the measured velocity vectors.

Relative cross sections for the production of selected ions, such as, e.g., N^+ or N_2^+, and of special processes such as $N_2 \rightarrow N^{q_1+} + N^{q_2+}$ can be obtained. A crucial point for the determination of cross sections is the detector efficiency that depends on the particular process. Consider, for example, the processes

$$He^+ + N_2 \rightarrow He^{(1-c)+} + N^{q_1+} + N^{q_2+} + n\,e^- \qquad (1)$$

with $n = q_1 + q_2 - c \geq 1$. In the experimental setup used the observation of such an event requires the detection of both ions and at least one electron. Currently we have no possibility of distinguishing between processes with a different number of ''free'' electrons n, and thus the fragmentation channels will subsequently be classified by the fragment charges q_1 and q_2. Clearly the probability P_e of detecting ''at least one'' electron depends on the number of free electrons n:

$$P_e(n) = 1 - (1 - \eta T)^n \qquad (2)$$

where $\eta \approx 0.8$ is the efficiency of the channeltron (including electronics) and $T = 0.9$ is the transmission of the grid in the electron path. Consequently the start probability is $P_e \approx 0.72$ for $n = 1$, $P_e \approx 0.92$ for $n = 2$, and essentially $P_e \approx 1$ for $n > 2$. Positive ions have to pass three grids before they are detected by the crossed-wire detector with an efficiency of $\epsilon \approx 0.4$ (MCP and x-y coincidence electronics). As a consequence of the crossed-wire structure it is possible to resolve particles which arrive ''at the same time'' on different wires. Due to this ''zero dead time'' feature the detection of both fragments may be considered as independent and the probability of observing at least one electron (out of n) together with both fragment ions is

$$P(n) = P_e(n)\,\epsilon T^3 \epsilon T^3 = \epsilon^2 T^6 P_e(n) \qquad (3)$$

which typically amounts to 8–8.5%.

Another important point is the finite size of the detector. The mutual Coulomb repulsion of the $N^{q_1+} + N^{q_2+}$ or $C^{q_1+} + O^{q_2+}$ system leads to considerable kinetic energies of the fragments ranging from 5 to 150 eV [34]. Depending on the locus of fragmentation and the initial direction of the molecular axis a part of the fragments will, especially at higher fragment energies, miss the active detector area. A Monte Carlo technique was used to estimate the losses introduced by the geometric and electronic detector characteristics for each fragmentation channel. The simulations show that in case of a separation field of 333 V/cm the spectrometer is close to the ideal of a 4π detector: the largest loss of $\approx 3\%$ was found for the $N^{3+} + N^{2+}$ channel.

The measured cross sections were corrected for both effects, the geometric and electronic characteristics and the detector efficiency of the particle detectors. Since the efficiencies are not exactly known, we estimate an uncertainty of 10% for each of the particle detectors. A determination of absolute cross sections additionally requires the precise knowledge of the projectile current and the target density, which is in general not easy to maintain. We therefore present only relative cross sections. The experiment requires the detection of at least one electron, so that pure capture processes, such as, e.g., $He^+ + CO \rightarrow He^0 + CO^+$, are not observed. Thus especially the single ionization cross section is clearly underestimated in this experiment. In the case of triple ionization, however, no pure capture processes occur and the probability of detecting at least one electron is close to 1. Therefore, the relative cross sections are normalized to the triple ionization yield. Since all reaction channels is measured simultaneously, the influence of the mentioned uncertainties are significantly reduced or even completely ruled out, such as, e.g., the influence of target density and the MCP efficiency. The main contributions arise from the statistical errors of the observed intensities and (especially in the case of σ_2/σ_3) the uncertainty in η. With a few exceptions (8% for σ_4/σ_3 in 250-keV $H^+ + N_2$, 7% for σ_4/σ_3 in 150-keV

TABLE I. Relative multiple ionization cross sections of diatomic molecules by H^+ and D^+ impact. The estimated experimental uncertainties are in general well below 4% (see text).

Collision	Energy (keV)	σ_2/σ_3 Expt.	σ_2/σ_3 Model	σ_4/σ_3 Expt.	σ_4/σ_3 Model
$H^+ + O_2$	50	9.1	12.88	0.064	0.035
	100	9.6	9.48	0.082	0.050
	150	11.1	8.92	0.085	0.054
	200	12.8	8.77	0.068	0.057
	250	14.0	8.78	0.066	0.059
	300	14.9	8.94	0.075	0.059
$H^+ + N_2$	50	5.5	9.50	0.051	0.049
	100	6.0	7.04	0.047	0.070
	150	6.7	6.59	0.055	0.079
	200	7.6	6.57	0.066	0.084
	250	8.1	6.74	0.075	0.084
	300	8.2	6.91	0.079	0.084
$D^+ + CO$	100	6.8	7.23	0.060	0.064
	150	5.5	6.06	0.067	0.079
	200	4.9	5.69	0.089	0.086
	250	4.9	5.57	0.090	0.089
	300	4.7	5.52	0.087	0.092
$D^+ + NO$	150	4.4	3.96	0.072	0.074
	200	4.1	3.71	0.092	0.082
	250	3.7	3.62	0.093	0.087
	300	3.8	3.59	0.097	0.090

TABLE II. Relative multiple ionization cross sections of diatomic molecules by He^+ impact. The estimated experimental uncertainties are in general well below 4% (see text).

Collision	Energy (keV)	σ_2/σ_3 Expt.	σ_2/σ_3 Model	σ_4/σ_3 Expt.	σ_4/σ_3 Model	σ_5/σ_3 Expt.	σ_5/σ_3 Model
$He^+ + O_2$	50	3.7	24.60	0.102	0.012		0.000
	100	2.9	6.36	0.176	0.078	0.008	0.002
	150	2.6	3.83	0.197	0.154	0.0124	0.009
	200	2.3	2.98	0.229	0.219	0.0152	0.021
	250	2.3	2.59	0.242	0.273	0.0197	0.036
	300	2.2	2.39	0.264	0.316	0.0247	0.052
$He^+ + N_2$	50	2.6	47.38	0.114	0.007		0.000
	100	1.8	10.15	0.194	0.048	0.0104	0.001
	150	1.6	5.71	0.219	0.098	0.0147	0.005
	200	1.5	4.25	0.233	0.142	0.0188	0.011
	250	1.6	3.58	0.238	0.181	0.0214	0.019
	300	1.6	3.22	0.235	0.213	0.0185	0.028
$He^+ + CO$	100	3.1	7.69	0.102	0.063		0.001
	150	2.7	4.66	0.146	0.121		0.007
	200	2.7	3.62	0.185	0.169	0.0103	0.015
	250	2.7	3.08	0.166	0.210		0.025
	300	2.8	2.81	0.183	0.243	0.0128	0.035
$He^+ + NO$	100	1.9	5.48	0.168	0.050	0.0128	0.002

$D^+ +$ NO, and 5% for σ_5/σ_3 in 100-keV $He^+ + N_2$ collisions) the estimated errors are in general well below 4%.

The experiment can clearly distinguish between different combinations of fragment charges, such as, e.g., $C^+ + O^{2+}$ and $C^{2+} + O^+$. The theoretical model discussed below, however, is only sensitive to the total charge Q of both fragment ions. Therefore, the cross sections for Q-fold ionization were derived by summing up the corresponding channels observed in the experiment. For example, the triple ionization of CO consists of the $C^+ + O^{2+}$ and $C^{2+} + O^+$ channels, and the fourfold ionization of N_2 of the $N^+ + N^{3+}$ and $N^{2+} + N^{2+}$ channels; channels with neutral fragments, such as, e.g., $N + N^{q+}$, are not detected.

For each electron-ion-ion coincidence the angle ϑ between the molecular axis and the direction of the projectile beam was derived from the measured velocity vectors. Thus the ionization cross sections can be studied as a function of the orientation of the molecular axis relative to the projectile beam. To simplify the study of the variation of the angular distributions with Q and with the projectile type and velocity as well as to simplify the comparison between the experiment and the model calculations, a dipole-type angular distribution (see the discussion in Sec. III) was fitted to the measured angle spectra. This somewhat crude approximation reflects at least the main characteristic features of the distribution by the anisotropy parameter β which can be compared with that computed in the model. Since for an isotropic distribution the number of dissociation events $N(\vartheta)$ with angles between ϑ and $\vartheta + d\vartheta$ is proportional to $\sin\vartheta$, the angular distribution was fitted by the expression

$$N(\vartheta) = N_0[1 + \beta P_2(\cos\vartheta)]\sin\vartheta. \tag{4}$$

using a nonlinear least-square algorithm to extract the anisotropy parameter β for each ionization degree.

III. RESULTS AND DISCUSSION

The experimental results presented in Tables I–IV are compared with our theoretical calculations which were performed within the SED model. The principles of the model are described in detail in the original papers by Russek and Meli [27] and Cocke [28]. The extension of the model with realistic calculations of the energy deposition and energy straggling is described in our previous publications [29,30]. Recently, we have developed a version of the SED model that can be applied when the projectile velocity is close to the Bohr velocity ($v \sim 1$) where the interaction cannot be considered as a perturbation [31]. This latest version is used in the present work. Since the description of the model including all necessary formulas is well documented in the cited papers we shall not repeat it here. Instead we briefly describe the main ideas and basic approximations used in the calculations.

The SED model is based on the assumption that multiple ionization may be considered as proceeding in two stages. First, the charged projectile interacting with the target electrons deposits some energy into the electronic system. At the second stage, when the projectile has already left the interaction region, a certain number of electrons are emitted by the ''hot'' target. The probability of n-electron emission is mainly determined by the corresponding volume of the avail-

TABLE III. The anisotropy parameter β of the angular distribution of fragment ions in multiple ionization of diatomic molecules by H^+ and D^+ impact. The experimental values β_{expt} and calculated values β_{calc} (see text) are shown for different degrees of ionization Q.

Collision	Energy (keV)	$Q=2$		$Q=3$		$Q=4$	
		β_{expt}	β_{calc}	β_{expt}	β_{calc}	β_{expt}	β_{calc}
$H^+ + N_2$	50	−0.26	−0.02	0.18	0.47		1.25
	100	−0.30	−0.08	0.16	0.30		0.98
	150	−0.26	−0.10	0.12	0.24		0.87
	200	−0.26	−0.10	0.09	0.20	0.12	0.81
	250	−0.29	−0.11	0.03	0.19		0.78
	300	−0.25	−0.11	−0.02	0.18	0.09	0.76
$H^+ + O_2$	50	−0.12	0.00	0.17	0.57		1.37
	100	−0.10	−0.05	0.22	0.41	0.33	1.14
	150	−0.07	−0.07	0.19	0.34	0.22	1.04
	200	−0.06	−0.09	0.15	0.30		0.96
	250	−0.06	−0.09	0.15	0.27		0.89
	300	−0.08	−0.10	0.11	0.26		0.85
$D^+ + CO$	100	0.13	−0.05	0.35	0.34	0.86	0.95
	150	0.13	−0.08	0.33	0.26	0.68	0.83
	200	0.10	−0.09	0.33	0.21	0.80	0.78
	250	0.10	−0.10	0.27	0.19	0.71	0.74
	300	0.22	−0.10	0.26	0.17	0.67	0.71
$D^+ + NO$	150	0.45	−0.14	0.39	0.15		0.91
	200	0.38	−0.15	0.35	0.11	0.85	0.82
	250	0.37	−0.16	0.35	0.08	0.99	0.77
	300	0.38	−0.16	0.31	0.06	0.88	0.72

able phase space. The SED model is semiempirical in the sense that it contains an adjustable parameter, the g factor, which characterizes the average square of the matrix element, describing the electron emission. In principle, the g factor can be adjusted separately for each colliding system and for each collision energy. However, our calculations show that it does not change much from system to system and depends only weakly on energy.

In accordance with the above description, first one calculates the energy deposited into the target electronic system, which is equal to the energy lost by the projectile in the collision with the molecule. For this calculation we have used the unitary convolution approximation (UCA) developed by Schiwietz and Grande [35], which permits one to calculate the impact parameter dependence of the mean energy loss provided the electronic density of the target is known. The latter was calculated in the Hartree-Fock approximation using the MOLPRO computer program [36–38], which was also used in the calculation of the ionization potentials for removing an electron from a molecule or molecular ion that are necessary for obtaining the ionization probabilities. The advantage of using the UCA is that this approximation takes into account higher-order corrections and therefore is applicable to the collisions of not very fast particles ($\kappa \sim 1$). Similarly, the straggling of the energy loss was calculated. The details of the application of the UCA to ion-molecule collisions are given in [31]. Knowing the deposited energy for each impact parameter one then calculates the probability of multiple ionization [29–31]. The corresponding cross sections are obtained by integration over all impact parameters. Since the time of the collision is much less than any rovibrational motion of the molecule, the latter

TABLE IV. The anisotropy parameter β of the angular distribution of fragment ions in multiple ionization of diatomic molecules by helium ion impact. The experimental values β_{expt}, and calculated values β_{calc}, (see text) are shown for different degrees of ionization, Q.

Collision	Energy (keV)	$Q=2$		$Q=3$		$Q=4$		$Q=5$	
		β_{expt}	β_{calc}	β_{expt}	β_{calc}	β_{expt}	β_{calc}	β_{expt}	β_{calc}
$He^+ + N_2$	50	−0.45	0.19	−0.19	1.08		1.85		1.99
	100	−0.50	−0.02	−0.23	0.45	0.29	1.22		1.81
	150	−0.52	−0.09	−0.24	0.22	0.30	0.81		1.49
	200	−0.51	−0.12	−0.25	0.11	0.30	0.58	1.11	1.23
	250	−0.50	−0.13	−0.25	0.04	0.30	0.45	1.20	1.05
	300	−0.50	−0.13	−0.23	0.00	0.33	0.36	1.33	0.91
$He^+ + O_2$	50	−0.38	0.06	−0.29	0.80	0.08	1.70		1.98
	100	−0.36	−0.10	−0.16	0.25	0.22	1.03	0.87	1.78
	150	−0.33	−0.16	−0.18	0.06	0.25	0.61	0.88	1.45
	200	−0.34	−0.18	−0.19	−0.03	0.21	0.39	0.94	1.17
	250	−0.33	−0.18	−0.17	−0.09	0.27	0.26	0.93	0.97
	300	−0.41	−0.18	−0.21	−0.12	0.32	0.18	1.02	0.83
$He^+ + CO$	100	0.22	−0.04	0.19	0.33	0.76	0.95		1.58
	150	0.30	−0.11	0.22	0.15	0.75	0.62		1.22
	200	0.32	−0.13	0.21	0.06	0.66	0.45	1.09	1.00
	250	0.35	−0.12	0.20	0.01	0.77	0.35		0.85
	300	0.34	−0.12	0.21	−0.02	0.63	0.27	0.80	0.75
$He^+ + NO$	100	0.18	−0.10	0.19	0.25	0.92	1.10	1.36	1.72

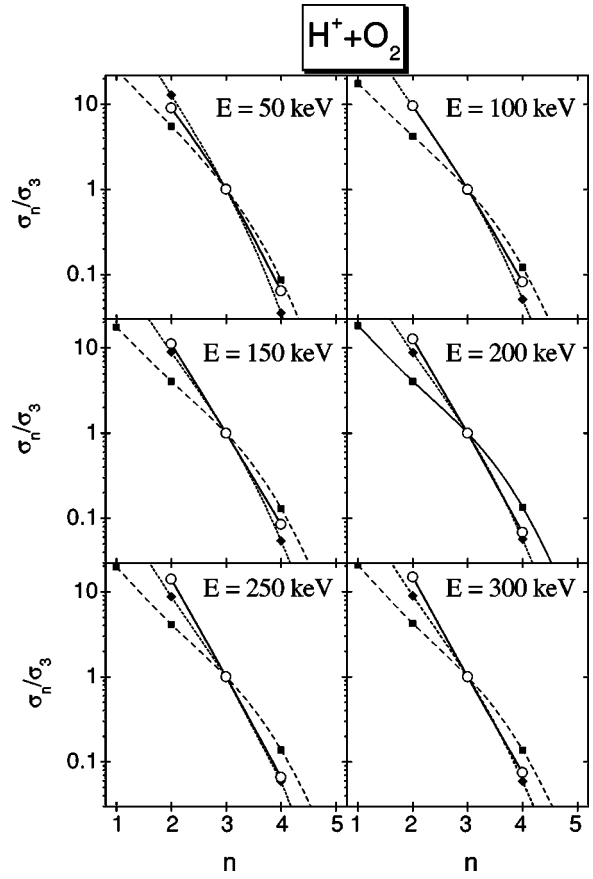

FIG. 1. Relative cross sections of n-fold ionization of O_2 molecules by proton impact at different collision energies. Open circles are the experimental results; black diamonds, calculations with $g=0.01$; black squares, calculations with $g=0.05$. The curves are drawn through the points to guide the eyes.

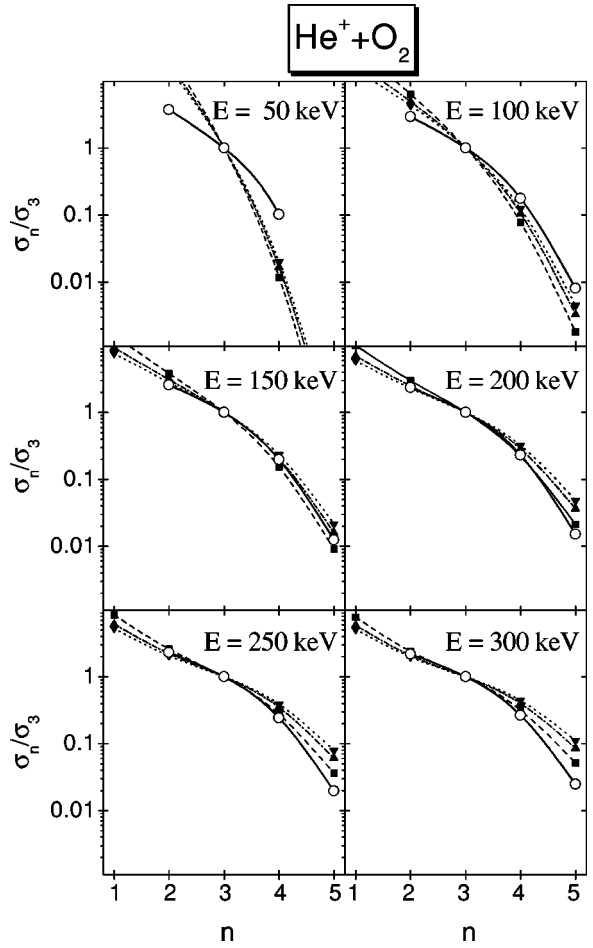

FIG. 2. Relative cross sections of n-fold ionization of O_2 molecules by He^+ impact at different collision energies. Open circles are the experimental results; filled symbols show the results of calculations with different g factors: $g=0.05$ (squares), $g=0.10$ (triangles pointing up), $g=0.15$ (triangles pointing down). The curves are drawn through the points to guide the eyes.

is considered as fixed in space during the collision. In this way the dependence of the multiple ionization cross section on the molecular orientation can be studied. The total cross section is obtained by averaging over all molecular orientations. Here we note that the SED model does not include ionization by electron capture. Within the model it is assumed that the degree of ionization is equal to the number of emitted electrons, $Q \equiv q_1 + q_2 = n$. In the experiment it is not always so [compare with Eq. (1)]. However, we shall ignore the capture process and assume that $Q=n$ in the comparison of the experimental data with the model calculations.

A. Cross section of multiple ionization

First we discuss the relative cross sections of multiple ionization. A comparison of the experimental and the calculated relative cross sections gives a good opportunity for choosing the g factor. As an example, in Fig. 1 we compare the experimental and theoretical relative cross sections normalized to the triple ionization cross section, i.e., the ratios σ_n/σ_3, for $H^+ + O_2$ collisions. The theoretical data are shown for two values of the g factor: 0.01 and 0.05. A comparison of these two calculations shows a general tendency: the smaller the g factor, the steeper is the curve representing the relative cross section as a function of the number of emitted electrons. The calculations with $g=0.01$ agree fairly well with the experimental ratios at practically all energies studied. A similar comparison for $He^+ + O_2$ collisions is shown in Fig. 2. For higher collision energies $E=150$–300 keV good agreement is achieved for $g=0.05$, with only a weak dependence on the exact value. However, for the energy of 100 keV and especially for 50 keV the theoretical curve is much steeper than the experimental one. Increasing the g factor makes the theoretical results closer to the experiment, but still the difference is too large, especially for $E=50$ keV. A possible explanation of the failure of our model at small velocities is that the electron capture mechanism, which is not included in our model, contributes considerably at these energies. Indeed, the experimental investigations by Rudd *et al.* [20] have shown that ionization of molecules by electron transfer to He^+ ions gives about 15% of the total ionization cross section at $E=250$ keV, but its contribution increases to 47% at $E=60$ keV. Unfortunately, there are no data on the capture rates for separate ionization channels. Hence, we are unable to correct our results for the capture contribution.

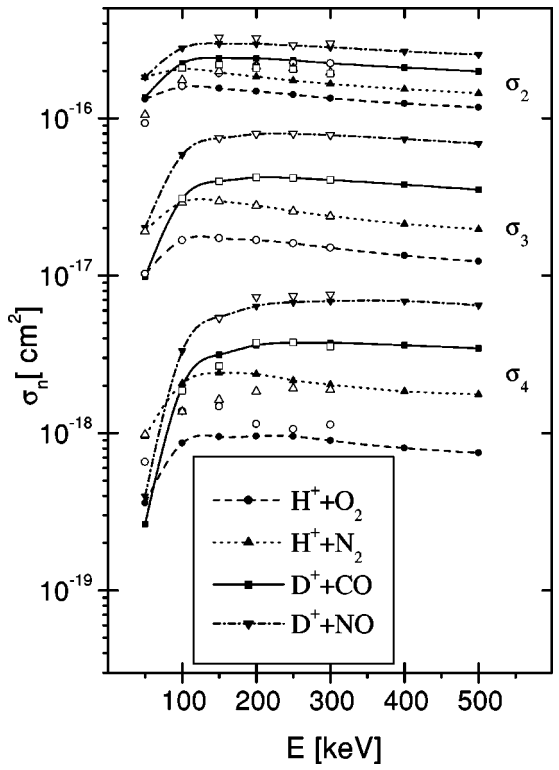

FIG. 3. Cross sections of *n*-fold ionization of O_2, N_2, CO, and NO molecules by proton and deuteron impact as functions of projectile energy. Filled symbols connected by curves represent the calculated cross sections (see text). Open symbols show the experimental data normalized to theoretical values of σ_3 at each energy. Molecules: O_2, circles; N_2, triangles pointing up; CO, squares; NO, triangles pointing down.

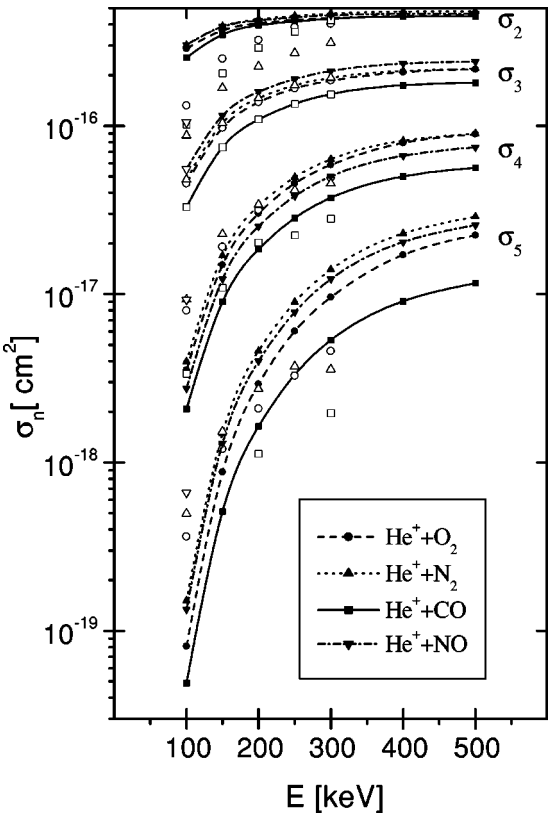

FIG. 4. Cross sections of *n*-fold ionization of O_2, N_2, CO, and NO molecules by He^+ impact as a function of He ion energy. Filled symbols connected by curves represent the calculated cross sections (see text). Open symbols show the experimental data normalized to theoretical values of σ_3 at each energy. Molecules: O_2, circles; N_2, triangles pointing up; CO, squares; NO, triangles pointing down.

The results of our calculations for other collision systems behave rather similarly. In the discussion below we refer to the theoretical calculations made with the following choice of the g factors: 0.01 for $p+O_2$, 0.05 for $p+N_2$, and $D^+ + CO,NO$. For collisions of He ions with $E>150$ keV the fitting gives $g=0.05$ for all molecules except N_2, where better results are obtained with $g=0.15$. For lower energies, $E \leqslant 150$ keV, the g factor should be larger for better agreement with experiment. In principle, one can fit the g factor also for these energies; however, it is probably not meaningful since electron capture, which becomes the dominant process at low energies, is not considered in the SED model. Thus the theoretical data presented below are calculated with the energy-independent g factors indicated above, but the results for the lowest energies should be considered with caution.

In Tables I and II we compare our experimental results with the calculations. For collisions with hydrogen ions the calculated ratios of the cross sections are in reasonable agreement with experiment for all considered energies (the average deviation is less than 20%). For He ions the agreement is reasonable for the energies $E>150$ keV. The exception is the case of $He^+ + N_2$ collisions. Here the experimental cross sections of double and triple ionization differ only slightly, while in the calculations the ratio σ_2/σ_3 is noticeably larger. The reason for this discrepancy is unclear. Part of this may be attributed to the fact that N_2^{2+} and $N^{2+}+N^0$ are not contained in the experimental cross sections. They only contain ion-ion events. (For O_2 this effect is small since less O_2^{2+} is produced.)

In Figs 3 and 4 we present the energy dependence of the cross sections of multiple ionization on an absolute scale for H^+ and He^+ collisions, respectively. The curves represent the results of our calculations. The experimental data are normalized at each energy to the theoretical triple ionization cross section. The energy dependence is reproduced rather well by the model calculation.

B. Orientation dependence of the cross sections

Anisotropy of the angular distribution of molecular fragments in dissociative ionization by a well directed beam of particles was predicted from very general symmetry arguments by Dunn [39]. If the dissociation takes place in a time small compared to a period of the molecular rotation, then the dissociation products will move along the direction of a molecular axis (axial recoil). Hence, for diatomic molecules measurements of the angular distribution of fragment ions provide the dependence of the ionization cross section on the orientation of the molecular axis with respect to the beam. When several electrons are removed from a molecule in a collision the multiply ionized molecular ion dissociates very quickly so that the axial recoil approximation holds. The

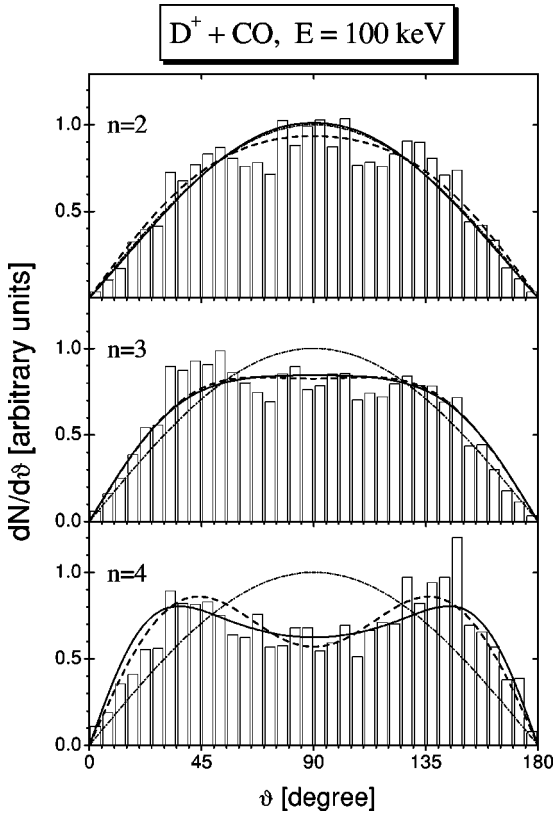

FIG. 5. Orientation dependence for the multiple ionization of CO molecules in collisions with 100-keV D^+ ions for *n*-fold ionization. The histograms show the experimental results. The dashed curves show the result of a fit by the dipole-type distribution (6). The solid curves are the results of the theoretical calculations within the SED model for $g=0.05$. The dot-dashed curve shows the sine distribution. All curves are normalized to the same area as the experimental histograms. ϑ is the angle between the ion beam direction and the molecular axis.

orientation dependence of the multiple ionization cross section was recently investigated both experimentally and theoretically (see [24–26,31,40] and references therein). It was found that the cross section of multiple ionization in the case when the molecular axis is aligned with the beam is considerably larger than when it is perpendicular to the beam. The effect increases with increase of the number of removed electrons *n*. According to the qualitative arguments presented in [31] we could expect a notable orientation effect for hydrogen and helium projectiles in the considered energy range for $n \geqslant 3$. Indeed, we have observed the orientation effect for all colliding partners.

From simple symmetry arguments it is clear that the angular distribution of molecular fragments in a multiple ionization - fragmentation process may be presented as

$$I(\vartheta) = I_0 \left(1 + \sum_L \beta_L P_L(\cos\vartheta) \right) \tag{5}$$

where ϑ is the angle between the direction of the fragmention velocity and the projectile beam direction, $P_L(x)$ are Legendre polynomials, and I_0 is a normalization constant. This form is a consequence of the axial symmetry of the

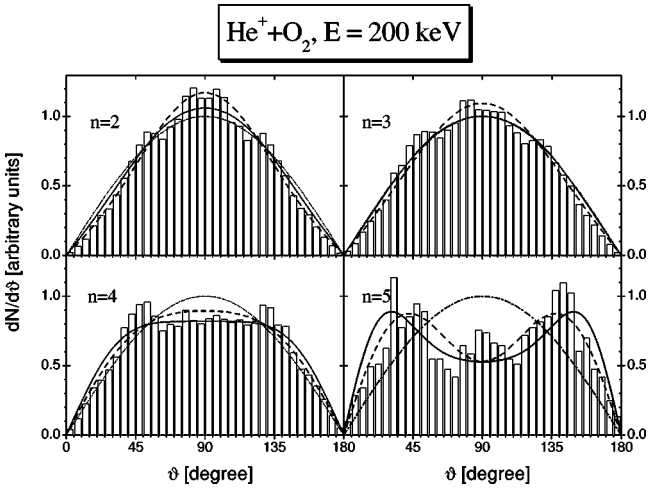

FIG. 6. The same as in Fig. 5 but for the collisions of 200-keV He^+ ions with O_2 molecules.

initial conditions: if we suppose that the directions of the molecular axes of the target molecules are randomly and uniformly distributed in space, then the only specified direction is the direction of the ion beam, thus the angular distribution of fragments should be axially symmetric with respect to this direction. For homonuclear diatomic molecules there is additional symmetry with respect to permutation of the atoms. This leads to the conclusion that only even values of *L* can contribute to the sum (5). For heteronuclear molecules odd-*L* terms can in principle contribute, describing a possible forward-backward asymmetry.

If the collision energy is high enough so that the Born approximation can be applied ($\kappa \ll 1$) then the multipole expansion of the Born amplitudes can be used and the contribution of different multipoles can be estimated [44,45]. The leading dipole term in the expansion gives rise to a differential cross section of the form

$$I(\vartheta) \approx I_0[1 + \beta P_2(\cos\vartheta)]. \tag{6}$$

This distribution coincides with the angular distribution of photoions in photoionization-dissociation of molecules [41]. For particle-impact ionization the dipole approximation should be valid only for high collision energies. Analysis of the double ionization of H_2 by proton impact [43] in the Born approximation leads to an expression containing terms proportional to $\cos^2\vartheta$ and $\cos^4\vartheta$ corresponding to terms $L=2$ and 4 in expression (5). However, the experimental results [43] in the energy region of about 1 MeV have not given a noticeable contribution of the $\cos^4\vartheta$ term.

As first discussed by Zare [44] and later confirmed by measurements for dissociative ionization of hydrogen molecules [45] and by calculations [42], the higher multipoles contribute considerably if the collision involves large momentum transfer. One can expect that for multiple ionization the typical momentum transfer increases with increase of the number of emitted electrons; therefore the higher-order multipole corrections to the simple dipole-Born approximation can be noticeable for higher degrees of ionization. In fact, model calculations of the orientation effect for multiple ionization of diatomic molecules by ion-impact [24,26] have

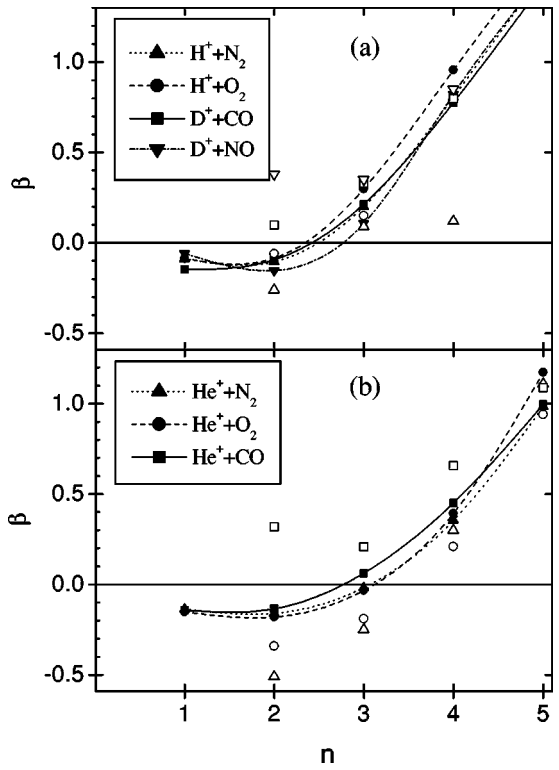

FIG. 7. Experimental and theoretical β values as function of the number of removed electrons n for collisions of 200-keV H^+ (a) and He^+ (b) ions with molecules. Filled symbols connected by lines represent the results of our calculations, the corresponding open symbols show our experimental results.

shown that for the highest observed degrees of ionization the angular distribution is quite sharply peaked at 0° and 180°, clearly indicating that nondipole corrections are necessary. In this case, the description of the angular distribution by expression (6) would be inappropriate.

In this work all measured angular distributions are fitted by the dipole-type expression [multiplied by $\sin\vartheta$, Eq. (4)] which reproduces surprisingly well the main features of the distribution. Since our main purpose was to study the dependence of the general characteristics of the orientation effect on the projectile type and velocity as well as on the target molecule properties, we made no attempt to extract more refined characteristics of the angular distribution such as β_4 and other higher multipole contributions. In Figs 5 and 6 we show examples of the angular distributions measured for 100-keV $D^+ + CO$ and 200-keV $He^+ + O_2$, respectively. In both figures a clear deviation from the sine distribution is seen for $n=3$ and especially for $n=4$ and 5. We note that for heteronuclear molecules the experimental data do not show any forward-backward asymmetry within the experimental uncertainty. In the same figures we show the fitted dipole-type distributions as well as the results of our calculations with the SED model. The model calculations agree well with the experimental data.

The fitting of expression (4) to the experimental angular distributions yields the β parameter which describes the anisotropy of the dissociation. The values of β derived from the fit are shown in Tables III and IV. In a recently published paper [31] we characterized the anisotropy of the theoretical distributions by the parameter $A=[\sigma(0°)-\sigma(90°)]/[\sigma(0°)+\sigma(90°)]$. If the distribution is close to the dipole-type one, then the β parameter can be expressed in terms of A:

$$\beta = 4A/(3-A). \tag{7}$$

Using the values of A calculated in the SED model we obtained the anisotropy parameter β by Eq. (7). The results are compared with the experimental data in Tables III and IV. We note here that the theoretical curves in many cases may be better fitted by the expression (5) with $L=2$ and 4. However, for comparison with the experimental β's we ignored the higher-multipole corrections. The β values from fitting the theoretical curves are very close to those obtained from Eq. (7).

For higher values of $n=4,5$ the agreement between theory and experiment is satisfactory. Only for proton impact with N_2 and O_2 are the experimental values for $n=4$ much smaller than the calculated ones. However, in these cases the cross section is very small and the observed number of events was not sufficient for a reliable determination of the β value. For lower n the calculated values underestimate the experimental data. In addition, the calculated anisotropy for $n=2$ is in all cases small and negative, while in the experiment it has different signs for different molecules and it is not so small. To make it clearer we plotted the results for 200-keV H^+ and He^+ collisions for all molecules as a function of the number of removed electrons (see Fig. 7). It is interesting that for the homonuclear molecules (N_2 and O_2) the anisotropy for double ionization is negative, while for the heteronuclear molecules (CO, and NO) it is positive. One can speculate that this difference is due to the contribution of electron capture. It is known that for capture as well as capture with ionization from homonuclear molecules the interference effect can play a significant role [46,47]. The effect arises because the two atoms in the molecule are identical and the corresponding amplitudes from the two centers interfere. This enhances the cross section when the molecule is perpendicular to the beam and thus makes the β value negative. This effect, absent in heteronuclear molecules, may explain the observed difference. In our model calculation the capture process is disregarded and the results for homonuclear and heteronuclear molecules are similar.

IV. CONCLUSIONS

We have presented the results of a systematic study of H^+, D^+, and He^+ ions colliding with various diatomic molecules in the energy range of 50–300-keV. Relative multiple ionization cross sections and their dependence on the orientation of the molecular axis are obtained. We have also presented the results of extensive calculations of the cross sections within the SED model. For all considered collision partners the anisotropy of the angular distribution of molecular fragments is clearly established, especially for the highest observed degrees of ionization. This confirms our theoretical predictions [31]. The similarity of the results obtained for all

molecules studied confirms the interpretation of the orientation effect as depending primarily on the spatial distribution of the electron density in the molecule. The individual properties of the particular molecular states or molecular structure have a minor influence on the fragment angular distributions. This explains the favorable comparison of the experimental data with calculations within a statistical model which disregards the details of molecular structure. However, the angular distributions for double ionization disagree with the predictions of the SED model. Here more refined calculations are necessary.

ACKNOWLEDGMENTS

This work was supported by the Deutsche Forschungsgemeinschaft (DFG), by the Ministry of Science and Technology, Croatia, and by the EU Infrastructure Cooperation Network HRPI-1999-40012 (LEIF). N.M.K. acknowledges the hospitality of Bielefeld University and the financial support by the DFG within the Mercator professorship program. Z.K. is grateful to Bielefeld University for hospitality and to DAAD for financial support.

[1] C.J. Latimer, Adv. At., Mol., Opt. Phys. **30**, 105 (1993).
[2] L.S. Solov'ev, R.N. Il'in, V.A. Oparin, and N.V. Fedorenko, Sov. Phys. JETP **15**, 459 (1962).
[3] R. Browning and H.B. Gilbody, J. Phys. B **1**, 1149 (1968).
[4] V.V. Afrosimov, G.A. Leiko, Yu.A. Mamaev, M.N. Panov, and M. Voiovich, Sov. Phys. JETP **38**, 243 (1974).
[5] F.B. Yousif, B.G. Lindsay, and C.J. Latimer, J. Phys. B **23**, 495 (1990).
[6] M.B. Shah and H.B. Gilbody, J. Phys. B **23**, 1491 (1990).
[7] M.E. Rudd, R.D. DuBois, L.H. Toburen, C.A. Ratcliffe, and T.V. Goffe, Phys. Rev. A **28**, 3244 (1983).
[8] S.L. Varghese, G. Bissinger, J.M. Joyce, and R. Laubert, Phys. Rev. A **31**, 2202 (1985).
[9] H. Knudsen, U. Mikkelsen, K. Paludan, K. Kirsebom, S.P. Møller, E. Uggerhøj, J. Slevin, M. Charlton, and E. Morenzoni, J. Phys. B **28**, 3569 (1995).
[10] V. Krishnamurthi, I. Ben-Itzhak, and K.D. Carnes, J. Phys. B **29**, 287 (1996).
[11] L.S. Solov'ev, R.N. Il'in, V.A. Oparin, and N.V. Fedorenko, Sov. Phys. JETP **18**, 342 (1964).
[12] F.B. Yousif, B.G. Lindsay, F.R. Simpson, and C.J. Latimer, J. Phys. B **20**, 5079 (1987).
[13] H.O. Folkerts, R. Hoekstra, and R. Morgenstern, Phys. Rev. Lett. **77**, 3339 (1996).
[14] H.O. Folkerts, F.W. Bliek, M.C. de Jong, R. Hoekstra, and R. Morgenstern, J. Phys. B **30**, 5833 (1997).
[15] H.O. Folkerts, T. Schlathölter, R. Hoekstra, and R. Morgenstern, J. Phys. B **30**, 5849 (1997).
[16] A. Lafosse, J.C. Houver, and D. Dowek, J. Phys. B **34**, 819 (2001).
[17] L.I. Pivovar, Yu.Z. Levchenko, and A.N. Grigor'ev, Sov. Phys. JETP **27**, 699 (1968).
[18] A.K. Edwards and R.M. Wood, J. Chem. Phys. **76**, 2938 (1982).
[19] I. Ali, R. Dörner, O. Jagutzki, S. Nüttgens, V. Mergel, L. Spielberger, Kh. Khayyat, T. Vogt, H. Bräuning, K. Ullmann, R. Moshammer, J. Ullrich, S. Hagmann, K.-O. Groeneveld, C.L. Cocke, and H. Schmidt-Böcking, Nucl. Instrum. Methods Phys. Res. B **149**, 490 (1999).
[20] M.E. Rudd, T.V. Goffe, A. Itoh, and R.D. DuBois, Phys. Rev. A **32**, 829 (1985).
[21] U. Werner, J. Becker, T. Farr, and H.O. Lutz, Nucl. Instrum. Methods Phys. Res. B **124**, 298 (1997).
[22] B. Siegmann, U. Werner, and H.O. Lutz, Aust. J. Phys. **52**, 545 (1999).
[23] U. Brinkmann, A. Reinköster, B. Siegmann, U. Werner, H.O. Lutz, and R. Mann, Phys. Scr. **T80**, 171 (1999).
[24] U. Werner, N.M. Kabachnik, V.N. Kondratyev, and H.O. Lutz, Phys. Rev. Lett. **79**, 1662 (1997).
[25] K. Wohrer and R.L. Watson, Phys. Rev. A **48**, 4784 (1993).
[26] C. Caraby, A. Cassimi, L. Adoui, and J.P. Grandin, Phys. Rev. A **55**, 2450 (1997).
[27] A. Russek and J. Meli, Physica (Amsterdam) **46**, 222 (1970).
[28] C.L. Cocke, Phys. Rev. A **20**, 749 (1979).
[29] N.M. Kabachnik, V.N. Kondratyev, Z. Roller-Lutz, and H.O. Lutz, Phys. Rev. A **56**, 2848 (1997).
[30] N.M. Kabachnik, V.N. Kondratyev, Z. Roller-Lutz, and H.O. Lutz, Phys. Rev. A **57**, 990 (1998).
[31] Z. Kaliman, N. Orlić, N.M. Kabachnik, and H.O. Lutz, Phys. Rev. A **65**, 012708 (2001).
[32] J. Becker, K. Beckord, U. Werner, and H.O. Lutz, Nucl. Instrum. Methods Phys. Res. A **337**, 409 (1994).
[33] U. Werner, J. Becker, T. Farr, and H.O. Lutz, Nucl. Instrum. Methods Phys. Res. B **124**, 298 (1997).
[34] B. Siegmann, U. Werner, R. Mann, N.M. Kabachnik, and H.O. Lutz, Phys. Rev. A **62**, 022718 (2000).
[35] G. Schiwietz and P.L. Grande, Nucl. Instrum. Methods Phys. Res. B **153**, 1 (1999).
[36] MOLPRO is an *ab initio* program written by H.J. Werner and P.J. Knowles with contributions from J. Almlöf, R. Amos, S. Elbert, K. Hampel, W. Meyer, K. Peterson, R. Pitzer, and A. Stone.
[37] H.J. Werner and P.J. Knowles, J. Chem. Phys. **82**, 5053 (1985).
[38] P.J. Knowles and H.J. Werner, Chem. Phys. Lett. **115**, 259 (1985).
[39] G.H. Dunn, Phys. Rev. Lett. **8**, 62 (1962).
[40] B. Siegmann, U. Werner, R. Mann, Z. Kaliman, N.M. Kabachnik, and H.O. Lutz, Phys. Rev. A **65**, 010704(R) (2001).
[41] J.L. Dehmer and D. Dill, Phys. Rev. A **18**, 164 (1978).
[42] R.J. Van Brunt, J. Chem. Phys. **60**, 3064 (1974).
[43] A.K. Edwards, R.M. Wood, M.A. Mangan, and R.L. Ezell, Phys. Rev. A **46**, 6970 (1992).
[44] R.N. Zare, J. Chem. Phys. **47**, 204 (1967).
[45] R.J. Van Brunt and L.J. Kieffer, Phys. Rev. A **2**, 1293 (1970).
[46] T.F. Tuan and E. Gerjuoy, Phys. Rev. **117**, 756 (1960).
[47] S.E. Corchs, H.F. Busnengo, R.D. Rivarola, and J.H. McGuire, Nucl. Instrum. Methods Phys. Res. B **117**, 41 (1996).